JACC: CARDIOVASCULAR INTERVENTIONS VOL. 14, NO. 12, 2021

STATE-OF-THE-ART REVIEW

Principles of Intravascular Lithotripsy for Calcific Plaque Modification

Dean J. Kereiakes, MD,[a] Renu Virmani, MD,[b] Jason Y. Hokama, PhD,[c] Uday Illindala, PhD,[c] Carlos Mena-Hurtado, MD,[d] Andrew Holden, MD,[e] Jonathan M. Hill, MD,[f] Sean P. Lyden, MD,[g] Ziad A. Ali, MD, DPhil[h]

ABSTRACT

A significant proportion of lesions treated with transcatheter interventions in the coronary and peripheral vascular beds exhibit moderate to severe calcific plaques known to portend lower procedural success rates, increased peri-procedural adverse events, and unfavorable clinical outcomes compared with noncalcific plaques. Adapted from lithotripsy technology used for treatment of ureterorenal calculi, intravascular lithotripsy (IVL) is a novel technique for the treatment of severely calcific plaque lesions that uses acoustic shockwaves in a balloon-based delivery system. Shockwaves induce calcium fractures, which facilitate stent expansion and luminal gain. In this review, the authors summarize the physics, preclinical and clinical data on IVL use in the coronary and peripheral vasculature, and future directions of IVL in transcatheter cardiovascular therapies. (J Am Coll Cardiol Intv 2021;14:1275–92) © 2021 The Authors. Published by Elsevier on behalf of the American College of Cardiology Foundation. This is an open access article under the CC BY-NC-ND license (http://creativecommons.org/licenses/by-nc-nd/4.0/).

Vascular calcification reduces arterial compliance and complicates both short- and long-term clinical outcomes following revascularization (1–3). Coronary and peripheral artery calcification are reported in 18% to 31% and 30% to 50% of percutaneous procedures, respectively (4–6). Common risk factors for vascular calcification include advanced age, diabetes mellitus, and chronic kidney disease (1,7,8).

Coronary artery calcification negatively affects outcomes of coronary interventions by impeding device crossing and stent apposition and expansion (4,5), causing delamination of drug-eluting polymer (6), and altering drug delivery and elution kinetics (9). Stent underexpansion is associated with subsequent stent thrombosis and/or the need for target lesion revascularization (10). Techniques for modifying coronary artery calcification, including noncompliant, cutting, and scoring balloons as well as atheroablative technologies (atherectomy), have inherent limitations. High-pressure balloon dilatation with noncompliant or specialty balloons may have insufficient force to fracture calcium and achieve vessel expansion and can lead to barotrauma-related dissection or perforation. Laser atherectomy remains unpredictable, and rotational or orbital atherectomy exhibits wire bias in its effect, which may result in eccentric "rut or trough" formation with little impact on the circumference of calcium (11). Peri-procedural complications, including slow flow, myocardial infarction, flow-limiting dissection, distal embolization, and perforation, are more frequent

From [a]The Christ Hospital and Lindner Research Center, Cincinnati, Ohio, USA; [b]Cardiovascular Pathology Institute, Gaithersburg, Maryland, USA; [c]Shockwave Medical, Santa Clara, California, USA; [d]Yale-New Haven Hospital, Yale University School of Medicine, New Haven, Connecticut, USA; [e]Auckland City Hospital, Auckland, New Zealand; [f]Royal Brompton Hospital, London, United Kingdom; [g]Cleveland Clinic, Cleveland, Ohio, USA; and the [h]Columbia University Medical Center, New York, New York, USA.
The authors attest they are in compliance with human studies committees and animal welfare regulations of the authors' institutions and Food and Drug Administration guidelines, including patient consent where appropriate. For more information, visit the Author Center.

Manuscript received December 3, 2020; revised manuscript received February 23, 2021, accepted March 16, 2021.

ISSN 1936-8798 https://doi.org/10.1016/j.jcin.2021.03.036

ABBREVIATIONS AND ACRONYMS

CT = computed tomography

EHL = electrohydraulic lithotripsy

ESWL = extracorporeal shock-wave lithotripsy

ISWL = intracorporeal shock-wave lithotripsy

IVL = intravascular lithotripsy

OCT = optical coherence tomographic

RVD = reference vessel diameter

VF = ventricular fibrillation

with the adjunctive use of atheroablative technologies compared with balloon alone (7,12,13).

Similarly, peripheral artery calcification restricts vessel expansion, resulting in a higher residual stenosis that reduces procedural effectiveness and may impair the antiproliferative effect of drug-coated balloons (14,15). Endovascular treatment with percutaneous transluminal angioplasty or stenting is associated with increased rates of dissection, perforation, and distal embolization and reduced long-term patency (16–18) in the presence of peripheral artery calcification. Although atherectomy has been shown to improve luminal diameter and reduce the need for bailout stenting, vascular complications including distal atheroembolization remain a significant challenge (19–21).

Intravascular lithotripsy (IVL) has emerged as a novel therapy for the treatment of vascular calcification. IVL is based on the established therapeutic strategy of using acoustic pressure waves to treat renal calculi, with specific modifications in delivery to address vascular calcium. These adaptations include the incorporation of lithotripsy emitters (source of acoustic pressure waves) on the shaft of a balloon angioplasty catheter that deliver localized pulsatile acoustic pressure waves circumferentially to modify vascular calcium (22,23). The safety and effectiveness of IVL have been reported across multiple clinical studies involving severely calcified coronary and peripheral artery disease (24–30) (Supplemental Tables 1 and 2). In this context, it is appropriate to review the fundamental principles and proposed mechanism(s) of action of IVL on vascular calcification on the basis of available in vitro and in vivo data.

HIGHLIGHTS

- IVL has emerged as a novel therapy for treatment of vascular calcification.
- IVL safely and effectively modifies calcified lesions via lithotripsy-driven fracture.
- Understand longer-term outcomes following IVL modification of vascular calcification.

USE OF ELECTROHYDRAULIC EXTRACORPOREAL AND INTRACORPOREAL LITHOTRIPSY

Since its introduction in the 1980s, extracorporeal shockwave lithotripsy (ESWL) has been used as a first line treatment for urolithiasis (22,31–33) and commonly uses electrohydraulic lithotripsy (EHL) to generate high-energy acoustic shockwaves for stone fragmentation (i.e., stone comminution). In EHL, a spark gap discharge between two electrodes results in the formation of an acoustic pressure wave within the transmitting fluid medium that expands spherically outwards from the emitter. Because the spark gap discharge is initiated outside the body during ESWL treatment, high-energy shockwaves are focused through a process of parabolic reflection (focusing) to concentrate their fragmenting impact on the stone within the renal system. Energy discharged from the spark gap results in the formation of a plasma vapor bubble, which immediately follows the initial acoustic shockwave. The rapid expansion and collapse of the vapor bubble, also known as a cavitation bubble, creates secondary shockwaves (34). A standard EHL shockwave pressure pulse lasts about 5 to 10 μs and consists of a near instantaneous peak positive component that generates compressive stress, followed by a longer duration negative pressure trough that generates tensile stress. The application of EHL in ESWL treatment is summarized in Supplemental Figure 1.

Shockwaves travel through soft tissue with minimal effect because of similar acoustic impedance characteristics of water and soft tissue (i.e., water, 1.5×10^6 kg/[m^2 · s]; kidney, 1.6×10^6 kg/[m^2 · s]; muscle, 1.7×10^6 kg/[m^2 · s]). Fracturing effects are observed when shockwaves encounter tissue with differing acoustic impedances, such as the transition from soft tissue to calcified tissue (acoustic impedance of bone, 7.8×10^6 kg/[m^2 · s]) (23,35). The mechanism by which shockwaves fracture kidney stones is attributed to stresses created by the peak positive and negative pressures generated during the procedure by multiple mechanisms, including compressive, spalling, superfocusing, shearing, and squeezing stresses (Supplemental Figure 2) (23,36). Compressive stress is directly related to the positive peak pressure amplitude. With ESWL treatment using EHL technology, positive peak pressures range from 30 to 110 MPa (~300 to 1,100 atm). Spall stress, which is tensile stress imparting a "pulling" force on the targeted stone, is directly related to the negative peak pressure amplitude. During ESWL treatment, negative peak pressures range from −8 to −15 MPa (~80 to 150 atm) (23,37,38). Cavitation bubble formation and collapse on the surface of kidney stones also

FIGURE 1 IVL Shockwave Generation

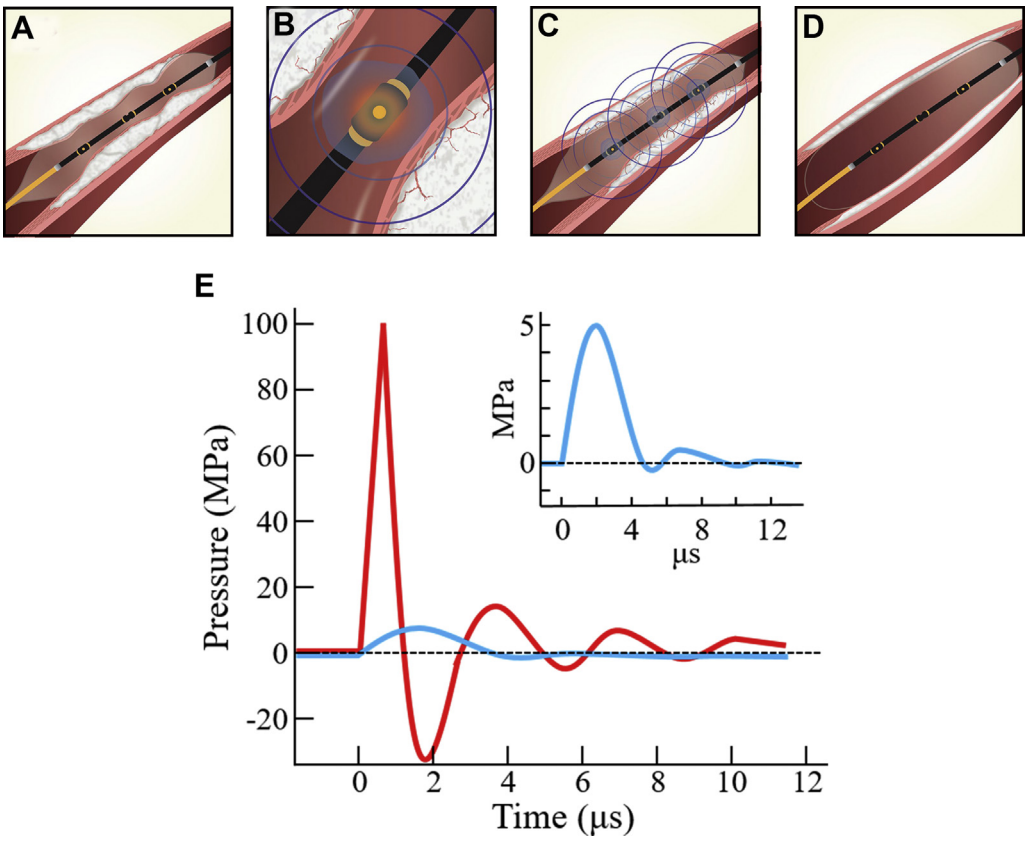

(A) The intravascular lithotripsy (IVL) balloon catheter is positioned across the target lesion and inflated to 4 atm. **(B)** Emitter spark gap discharge produces compressive shockwaves that emanate spherically outward; vapor bubble formation is contained with the integrated balloon. **(C)** IVL shockwaves affect superficial and deep calcium. **(D)** After IVL therapy is delivered, the balloon is inflated to 6 atm prior to deflation. **(E)** Superimposed IVL **(blue)** and extracorporeal shockwave lithotripsy **(red)** waveforms. Note the contrast in positive and negative peak pressures between the two electrohydraulic lithotripsy technologies. Representative IVL waveform demonstrating positive peak pressure of about 5 MPa with minimal negative peak pressure generation **(inset)**.

contributes to fragmentation. Cavitation is induced by the trailing peak negative pressure wave generated during ESWL treatment and results in microjet formation (high-velocity fluid spikes) that contribute to stone fragmentation through shearing as well. Microjets and heat generation created through cavitation may be associated with soft tissue damage, including abdominal wall dissection, perforation of the colon, hepatic hematoma, and major disruption of renal vasculature (23,39,40).

EHL technology has also been adapted for endoscopic treatment of bladder, ureteral, and kidney stones in situations in which ESWL is less effective (i.e., patients with morbid obesity, lower pole stone location). During intracorporeal shockwave lithotripsy (ISWL), the emitter is located at the tip of a catheter, which is passed through an endoscope inserted into the urethra and positioned in close proximity to the stone, thereby decreasing the energy required for stone fragmentation and allowing unfocused delivery of shockwave pressure pulses. Smaller ISWL probes have allowed improved access to anatomically challenging stone locations. The effect of ISWL acoustic shockwaves remain consistent: stone fracture with safe propagation through soft tissue. However, the margin of safety for ISWL is narrow because of direct exposure of the activated emitter and cavitation bubbles to the surrounding tissue, which may increase the risk for tissue injury with consequent perforation, hemorrhage, and mucosal denudation (39,41,42). Although risks for thermal injury or tissue damage from cavitation are

TABLE 1 Electrohydraulic Lithotripsy Characteristics in ESWL, ISWL, and IVL

	ESWL	ISWL	IVL
Emitter location	Extracorporeal	Intracorporeal	Intravascular
Focused or unfocused lithotripsy	Focused	Unfocused	Unfocused
Peak positive acoustic pressure (MPa)*	30-110	3-6	~5
Peak negative acoustic pressure (MPa)*	−8 to −15	−1 to −4	−0.3
Energy flux density (mJ/mm^2)	0.1 to 3.0	–	~0.0086
Penetration depth of acoustic pressure wave (mm)	~150	~10	3-7
Primary mechanisms of calcium fracture	Compression and tensile stress, cavitation, spall, squeezing, superfocusing	Compression and tensile stress, cavitation	Compression stress

*1 MPa = 9.8 atm.
ESWL = extracorporeal shockwave lithotripsy; ISWL = intracorporeal shockwave lithotripsy; IVL = intravascular lithotripsy.

mitigated by features that shield healthy soft tissue from direct contact with the vapor bubble and cavitation, careful attention to probe placement remains critical for preventing tissue injury with ISWL (42).

PRINCIPLES OF SHOCKWAVE IVL

IVL SYSTEM AND PROCEDURE. The Shockwave IVL catheter (Shockwave Medical, Santa Clara, California) is a single-use, sterile, disposable catheter that contains multiple spark gap-based lithotripsy emitters along the shaft of an integrated balloon (Supplemental Figure 3). The IVL catheter is introduced into the target vessel over a 0.014-inch guidewire and is positioned across the target lesion using balloon marker bands as visual guides. The catheter is connected using a connector cable to the generator that is programmed to deliver a pre-defined number of pulses (according to IVL catheter type) at a rate of 1 pulse/s. The integrated balloon, filled with a 50:50 saline/contrast mixture (ions are required for spark generation), is inflated to subnominal pressure (4 atm) to provide apposition with the vessel wall, which creates an effective fluid-tissue interface with similar acoustic impedances to facilitate efficient transmission of shockwave energy to vascular tissue.

ADAPTATION OF EHL TECHNOLOGY FOR INTRAVASCULAR USE. Although EHL spark gap technology was leveraged for use in IVL (43), the unique challenges posed by vascular calcium necessitated adaptations for safe and effective intravascular treatment. Three key modifications were incorporated for IVL: 1) IVL pressure waves deliver tissue-safe positive and minimal peak negative pressure pulses, which allow sufficient compressive force to modify vascular calcium while mitigating soft tissue injury due to excessive cavitation or tensile stress; 2) pressure wave emitters are enclosed within an inflated, fluid-filled balloon to mitigate thermal injury; and 3) multiple emitters are arranged in series along the shaft of the catheter for longitudinal treatment of the calcified vessel.

IVL ACOUSTIC PRESSURE WAVEFORM MODIFICATION. IVL emitters produce electric sparks that create vapor bubbles in the surrounding fluid medium within the integrated balloon. IVL produces low levels of electric energy, which leads to the formation and rapid expansion of vapor bubbles, which result in acoustic pressure waves that radiate circumferentially and transmurally in an unfocused manner (**Figure 1A, Video 1**). By modifying the pulse width applied to the emitters, the IVL acoustic pressure wave achieves a relatively low positive peak pressure of approximately 5 MPa (~50 atm) with a negligible peak negative pressure (about −0.3 MPa or −3 atm) compared with ESWL (**Figure 1B**). Similar to ESWL, IVL shockwaves propagate through soft tissue with minimal effect. The leading edge of the shockwave imparts compressive stress once calcium is encountered and is the primary mechanism of calcium fracture with IVL. Unlike ESWL, IVL shockwaves produce negligible peak negative pressures, and the resulting tensile stress (about −0.3 MPa or −3 atm) remains well below the threshold associated with tissue damage (44), thus mitigating cavitation-induced tissue injury. The unfocused nature of IVL shockwaves results in several orders of magnitude lower energy flux density (the amount of acoustic energy per unit area) compared with ESWL. As the goal is calcium fracture (as opposed to pulverization with ESWL), and IVL shockwaves are initiated in close proximity to the target vascular calcium, much less energy is required for IVL (compared with ESWL). Thus, IVL energy flux density is adequate for vascular calcium fracture while limiting the potential for soft tissue injury associated with higher energy levels. EHL device parameters are summarized in **Table 1**.

INTEGRATED IVL BALLOON. Integration of a semi-compliant balloon with emitters on the shaft offers several advantages during IVL treatment. First, the balloon provides a mixture of contrast and saline to dissipate heat generated during the formation of vapor bubbles (Supplemental Figure 4) and shields the emitters from direct contact with the vessel wall. Integrated periodic deflation of the balloon between pulse delivery cycles also serves to dissipate heat and remove residual gas bubbles through fluid evacuation

while allowing tissue reperfusion to mitigate ischemia. Second, the integrated balloon provides mechanical support and stabilization that serves to minimize any tissue deformation during IVL treatment. Third, the integrated balloon is thin and acoustically transparent to provide efficient fluid-to-tissue transmission and effective coupling of IVL pressure pulse propagation from emitter to vascular wall. The importance of such coupling was demonstrated in a series of experiments in which Ultracal 30 gypsum rings were subjected to IVL shockwaves under varying balloon-wall apposition conditions. Ultracal 30 gypsum does not account for micromorphological conditions encountered in vivo (i.e., lipid and fibrous tissue) but does mimic the acoustic properties of calcium encountered in vivo and provides a reproducible model of calcium fracture in lithotripsy research (45,46). Greater ring fracturing was observed when the IVL balloon was appropriately sized to ensure balloon-wall apposition (Supplemental Figure 5). Adequate balloon-vessel wall apposition is achieved at the subnominal pressure of 4 atm, thus minimizing barotrauma normally associated with high-pressure balloon angioplasty (47–49).

EMITTER ALIGNMENT AND ENERGY DISTRIBUTION. IVL uses multiple emitters outside the guidewire lumen, arranged in series along the length of the balloon segment. IVL emitters are positioned as diametrically opposing pairs (180° from each other) and emit spherical energy profiles that are nearly symmetrical mirror images along the balloon edge. These emitters are arranged into channels, with each channel pulsing at 1 Hz. Three IVL catheter models are currently available, allowing variation in vessel diameter and length of treatable segments associated with coronary and peripheral vessels (**Table 2**).

Signature patterns of peak acoustic pressures along the length of the IVL catheter align with the location of the emitters. The distribution of acoustic energy for each catheter type is shown in **Figure 2**. When channels are activated, the IVL paired emitters create acoustic pressure waves that radiate in a circumferential and transmural fashion to disrupt vascular calcium. As IVL delivers unfocused lithotripsy, the effective radiating pressure effect decreases with distance from the emitter. For the Shockwave M^5 catheter, note that the center channel has a single emitter; consequently, the activation energy for the center channel is not shared across 2 emitters, resulting in a greater peak acoustic pressure relative to the proximal and distal channels where energy is shared across two emitters. Understanding the energy distribution profile for each IVL catheter model helps the operator align the greatest acoustic pressure with the area of maximum calcium burden.

TABLE 2 Intravascular Lithotripsy Catheter Specifications

	Shockwave M^5	Shockwave S^4	Shockwave C^2
Use	Peripheral	Peripheral	Coronary
Diameter (mm)	3.5–7.0	2.5–4.0	2.5–4.0
Sheath compatibility	6 F (3.5–6.0 mm), 7 F (6.5–7.0 mm)	5 F	6 F*
Guidewire compatibility	0.014 inch	0.014 inch	0.014 inch
Length (mm)	60	40	12
Working length (cm)	110	135	138
Crossing profile (inches)	0.054–0.073	0.048–0.050	0.044–0.047
Pulse frequency (pulses/s)	1	1	1
Maximum number of pulses per catheter	300	160	80
Number of channels	3	2	1

*Guide catheter.

IVL CATHETER SIZING AND EMITTER ALIGNMENT. The importance of IVL balloon sizing and emitter alignment was observed in a post hoc analysis of the Disrupt PAD II (Shockwave Lithoplasty DISRUPT Trial for PAD) study, highlighting the impact of optimal IVL technique on 12-month primary patency when used as stand-alone therapy in superficial femoral and popliteal arterial segments (29). The optimal technique was

FIGURE 2 Acoustic Peak Pressure Aligns With Emitter Location

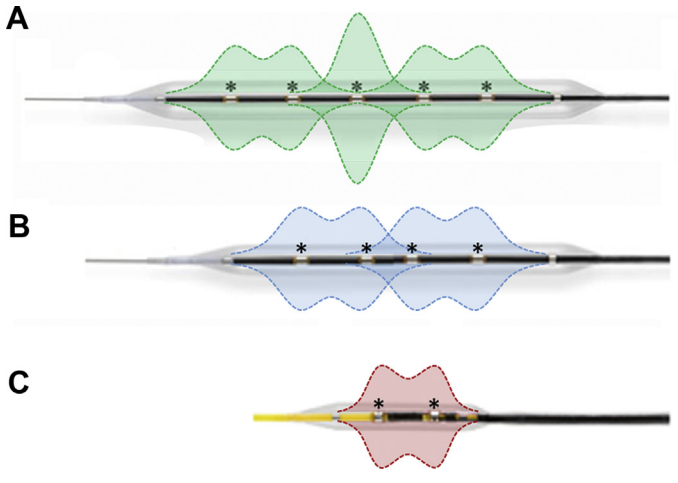

Shaded areas represent acoustic pressure profiles for the **(A)** Shockwave M^5, **(B)** Shockwave S^4, and **(C)** Shockwave C^2 intravascular lithotripsy catheters. Note that peak acoustic pressures are aligned with emitter location **(*)**.

FIGURE 3 Representative Micro-Computed Tomographic Images Before and After IVL Treatment

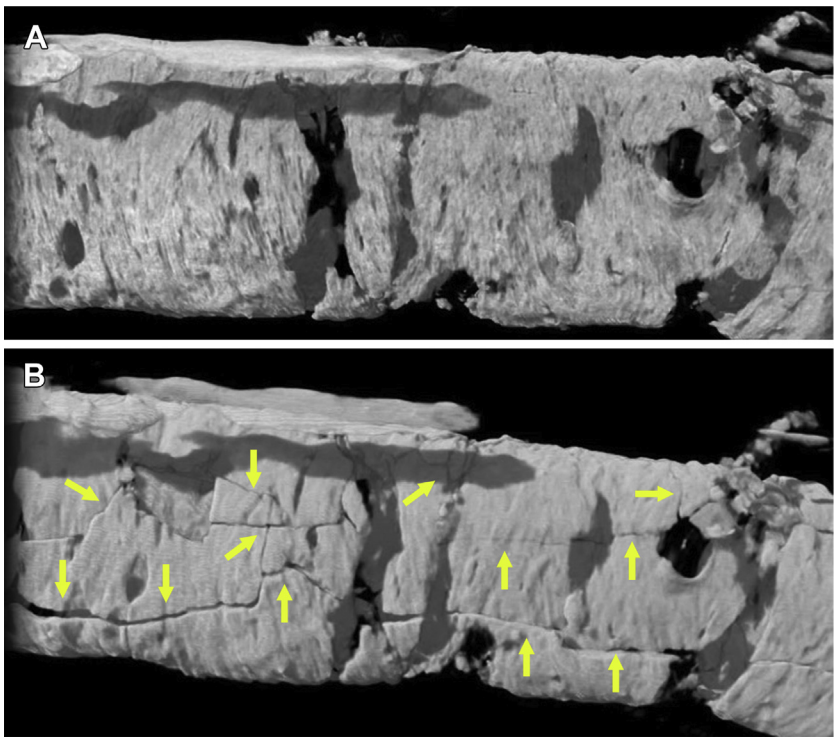

Abluminal view of the left distal femoral artery demonstrating predominantly medial calcification. **(A)** Before intravascular lithotripsy (IVL) treatment and **(B)** after IVL treatment. Circumferential, transverse, and longitudinal calcium fractures were observed following IVL treatment **(arrows)**.

defined as correct balloon sizing and avoidance of therapeutic miss (Supplemental Figures 6A to 6C). Balloon sizing was calculated as the ratio of the IVL balloon to reference vessel diameter (RVD), with a ratio ≥1 defined as appropriate balloon sizing. Therapeutic miss was defined as failure to provide full lithotripsy treatment at an overlap segment or at the proximal or distal lesion location. Use of optimal IVL technique was associated with significant improvement in 12-month primary patency and a reduction in clinically driven target lesion revascularization (Supplemental Figure 6D). Importantly, no increase in adverse events was observed when IVL balloon size exceeded RVD. On the basis of these findings, the Shockwave M^5 and S^4 IVL instructions for use recommend IVL catheter sizing of 1.1:1 with target vessel RVD, in addition to sufficient balloon overlap when treating long lesions to ensure optimal results. The instructions for use for the Shockwave C^2 IVL catheter (currently approved for use outside the United States) recommend IVL balloon sizing of 1:1 with target vessel RVD.

COMPARISON OF IVL SHOCKWAVE AND ULTRASOUND PROPERTIES. In contrast to IVL shockwaves, diagnostic (i.e., imaging) and therapeutic (i.e., deep tissue heating or tissue ablation) ultrasound waves propagate through tissue with high frequency (1 to 12 MHz) and with equal positive and negative pressure amplitudes (Supplemental Table 3). Ultrasound waves are absorbed or reflected by tissues of differing acoustic impedance. Energy from absorbed ultrasound waves results in heat generation, with higher energy ultrasound leading to tissue ablation (50,51). Ultrasound is also associated with cavitation bubble-induced injury resulting from the oscillating negative pressure cycle inherent to ultrasound waveforms (50,51). As IVL shockwaves have neither similar frequencies nor sinusoidal oscillations compared with ultrasound, the potential for thermal injury is less. Thus, both negligible negative pressures and fluid-filled balloon integration combine to reduce the risk for cavitation bubble-induced injury during IVL treatment. Waveform characteristics for IVL and ultrasound are shown in Supplemental Table 3.

FIGURE 4 Histological and Micro-Computed Tomographic Imaging After Intravascular Lithotripsy Treatment

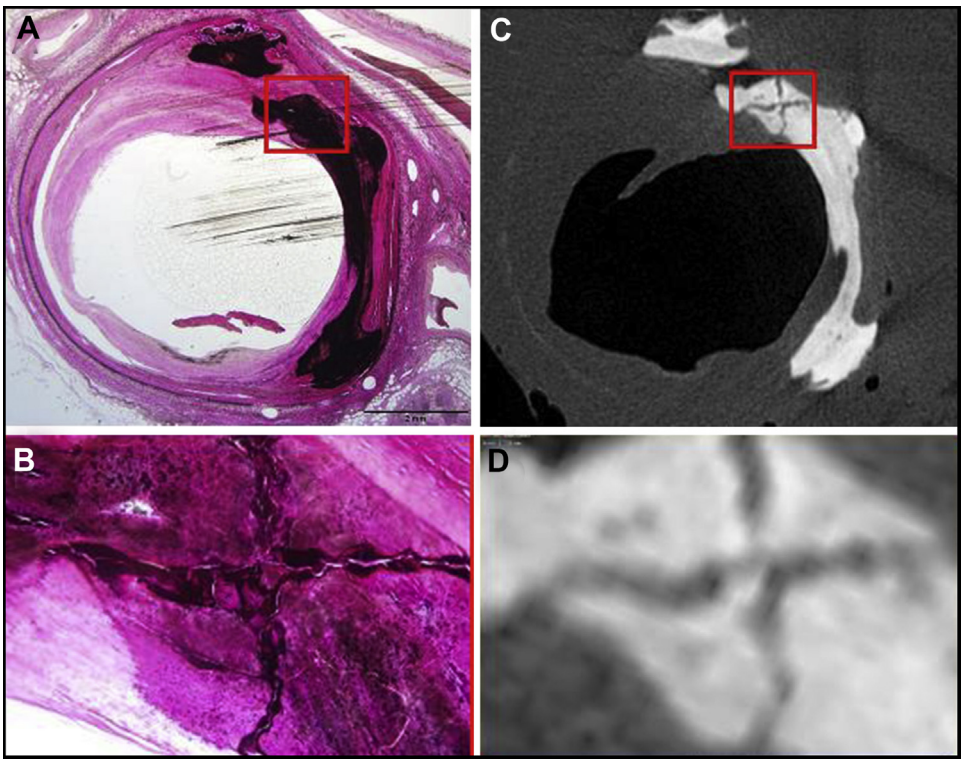

Cross-sectional histological Exakt ground section **(A)** matched with the micro–computed tomographic cross-sectional image **(C)**. Both sections show cross-shaped cracks highlighted by **red boxed areas**, which are shown at high-power magnification **(B,D)**.

IVL CALCIUM MODIFICATION IMPROVES VASCULAR COMPLIANCE

MICRO–COMPUTED TOMOGRAPHIC AND HISTOPATHOLOGIC VISUALIZATION OF IVL-MEDIATED CALCIUM FRACTURE. An independent cadaveric study using micro-computed tomography (CT) and histopathology was performed on heavily calcified, excised human superficial femoral arteries to evaluate the mechanism(s) by which IVL affects superficial and deep calcium (CVPath Institute, Gaithersburg, Maryland). The test model consisted of fresh-frozen human cadaveric femoral arteries (n = 6) with demonstrated presence of intimal and medial calcium. In contrast to formalin-preserved cadaveric arteries, fresh-frozen cadaveric arteries retain much of the tissue properties necessary for clinically relevant vascular interventions. Arteries were cannulated and placed in the lumen of a closed chamber with a tubular elastic balloon cuff to simulate perivascular pressure. The Shockwave IVL 60-mm catheter was used with balloon sizes ranging from 5.5 to 7.0 mm. The balloon size and deployment were based on measurements of the vessel cross-sectional area using baseline micro-CT. At the time these experiments were performed (2018), the 60-mm IVL catheter's maximum output was 180 pulses. Therefore, IVL treatment using 180 pulses was delivered at 4-atm balloon pressure in each artery per the device instructions for use. Pulses were delivered at 1 pulse per second, with 30 pulses per cycle followed by balloon deflation for 10 seconds between cycles. Six cycles were delivered for a total of 180 pulses. Micro-CT was performed before and after IVL treatment. Longitudinal and cross-sectional images were generated to evaluate the effect of IVL on calcium. For histopathology, nondecalcified arteries were embedded in Spurr's resin, sawed, and ground using the Exakt method to create sections varying in thickness from 50 to 90 μm and stained with hematoxylin and eosin.

Micro-CT demonstrated circumferential, transverse, and longitudinal calcium fractures with involvement of both superficial and deep layers of the vessels following IVL treatment (Figure 3).

FIGURE 5 Histological Examination of a Human Cadaveric Superficial Femoral Artery Following Intravascular Lithotripsy Treatment

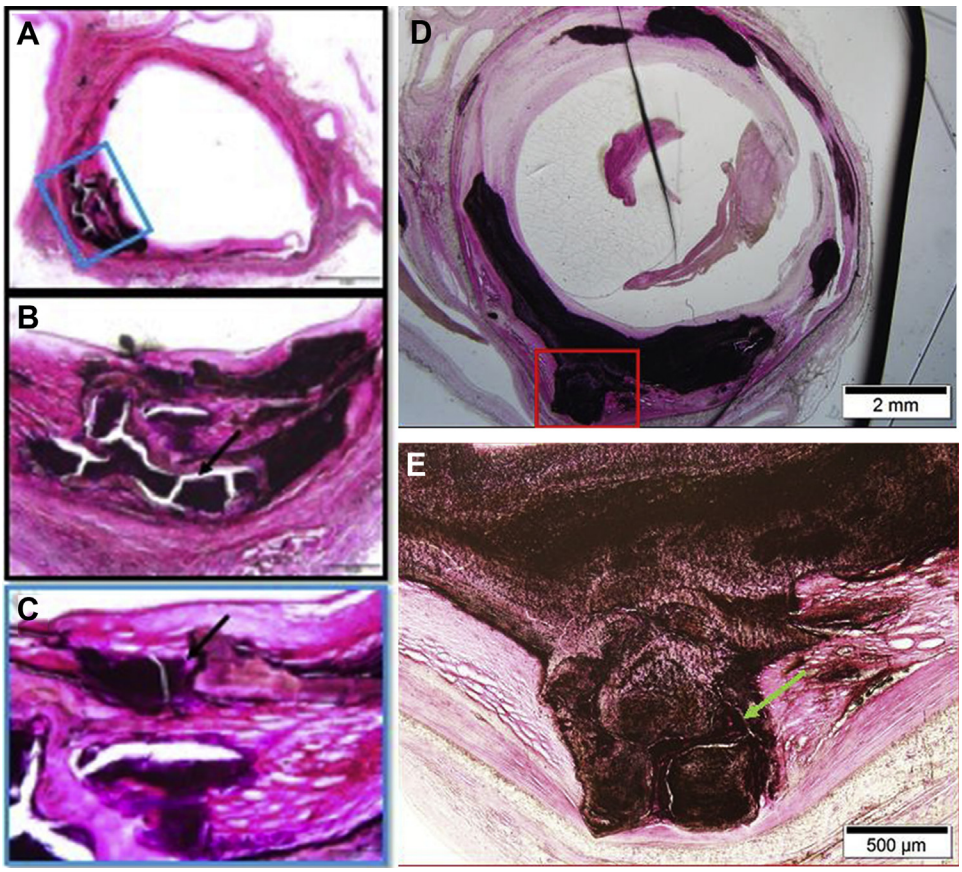

Hematoxylin and eosin–stained sections demonstrate **(A)** multiple fractures of superficial and deep calcification. **(B) Blue boxed area in A** is shown at higher magnification. **(C)** Further magnification demonstrates microfractures **(arrow)** not readily visible at lower magnification. **(D)** Histological Exakt section demonstrates an area of fracture at the tip of the intimal calcium extending into the adventitia. **(E) Red boxed area in D** is shown at higher magnification, demonstrating fracture **(arrow)**.

Coregistration of micro-CT and histopathology identified multiple full-thickness and deep calcium fractures that did not traverse to the luminal surface. Magnified histopathologic images revealed microfractures involving both the superficial (Figure 4) and deep layers (Figure 5) of a heavily calcified lesion.

OPTICAL COHERENCE TOMOGRAPHIC VISUALIZATION OF IVL-INDUCED CALCIUM FRACTURE. The Disrupt CAD I (Shockwave Coronary Rx Lithoplasty® Study), Disrupt CAD II (Shockwave Coronary Lithoplasty® Study), and Disrupt CAD III (Disrupt CAD III With the Shockwave Coronary IVL System) optical coherence tomographic (OCT) substudies (25,30,52) and Disrupt PAD II OCT subanalyses (53) demonstrated calcium fracture following IVL treatment similar to the micro-computed tomographic and histopathologic findings from cadaveric studies. Consistent observations across these OCT substudies included the following: 1) the mechanism of luminal gain following IVL treatment is calcium fracture, without the need for high-pressure balloon dilatation; 2) IVL results in circumferential and longitudinal calcium fracture; and 3) IVL treatment improves vessel compliance and facilitates stent expansion in calcified coronary arteries. In this clinical setting, an increase in arterial luminal area is evident following IVL, when the balloon is inflated to the same pressure. Although differentiation between intimal and medial calcification can be observed in peripheral vessels, the medial layer becomes attenuated in advanced coronary artery disease (54), and the distinction between intima and media on OCT imaging is challenging. Medial calcification, which is

FIGURE 6 OCT Imaging in Peripheral and Coronary Arteries After IVL Treatment

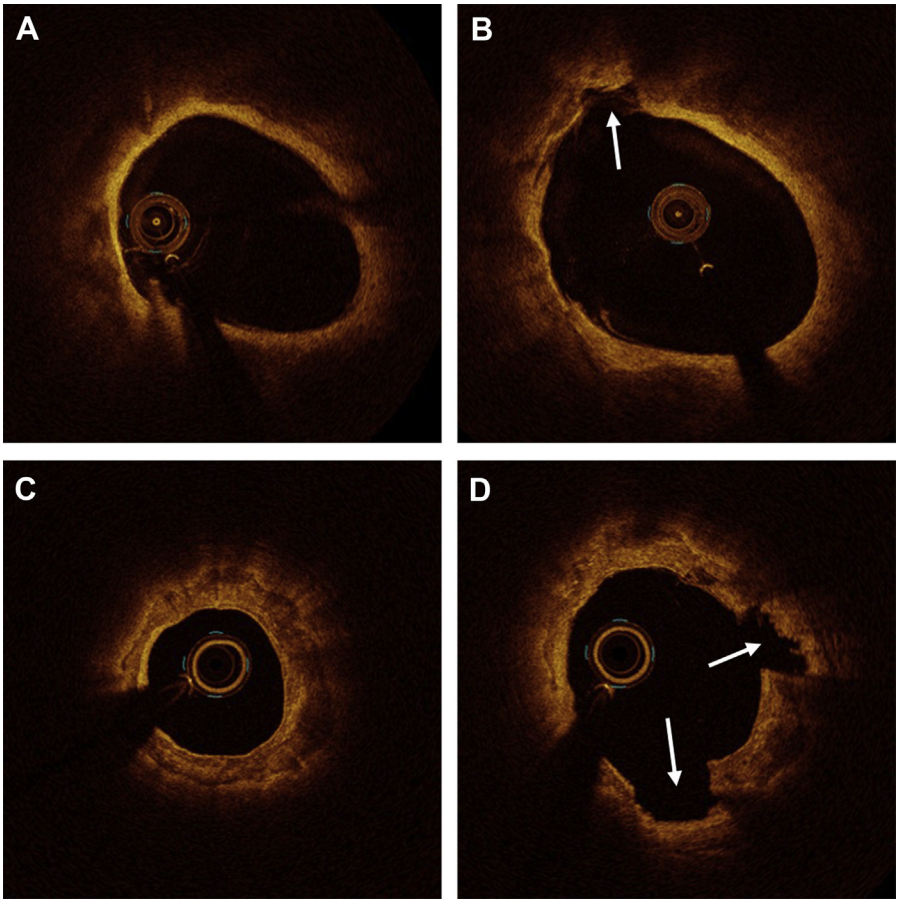

(A) Cross-sectional optical coherence tomographic (OCT) image acquired before intravascular lithotripsy (IVL) demonstrates 274° calcium arc and luminal area of 9.8 mm^2 in the distal superficial femoral artery. **(B)** Post-IVL OCT image demonstrates calcium fractures **(arrows)** and large luminal area gain to 12.6 mm^2. **(C)** Cross-sectional image acquired before IVL demonstrates 360° calcium arc and luminal area of 3.2 mm^2 in the mid-right coronary artery. **(D)** Post-IVL OCT image demonstrates calcium fractures **(arrows)** and large luminal area gain to 6.9 mm^2.

common in peripheral artery disease, is not observed in coronary arteries. Therefore, the designations "superficial" and "deep" as they relate to calcium location may be more appropriately applied to coronary calcification. Regardless of anatomic differences, the safety and effectiveness of IVL in calcified peripheral and coronary vessels have been consistently demonstrated across peripheral and coronary vascular beds (25,30,55,56). Data are limited regarding the effect of IVL treatment on eccentric and nodular calcium. Likewise, OCT imaging of IVL treatment in peripheral arteries is limited, as intravascular ultrasound is more commonly used in patients with peripheral artery disease. However, angiographic data from a 336 patient-level pooled analysis from the Disrupt PAD I (Safety and Performance Study of the Shockwave Lithoplasty System), Disrupt PAD II, Disrupt PAD III (Shockwave Medical Peripheral Lithoplasty System Study for PAD), Disrupt BTK (Safety and Feasibility of the Shockwave Lithoplasty® System for the Treatment of Peripheral Vascular Stenosis), and Disrupt CFA peripheral artery studies demonstrated no difference in final diameter stenosis between eccentric and concentric lesions. Similarly, in coronary arteries, patient-level pooled angiographic data from Disrupt CAD I and Disrupt CAD II (57) demonstrated similar angiographic outcomes and complications between eccentric and concentric lesions. Furthermore, a tertile analysis stratified by calcium burden in the Disrupt CAD I OCT substudy demonstrated similar stent expansion (>100%) at the site of maximum

FIGURE 7 OCT Imaging Demonstrates Longitudinal and Deep Calcium Fractures After Coronary IVL Treatment

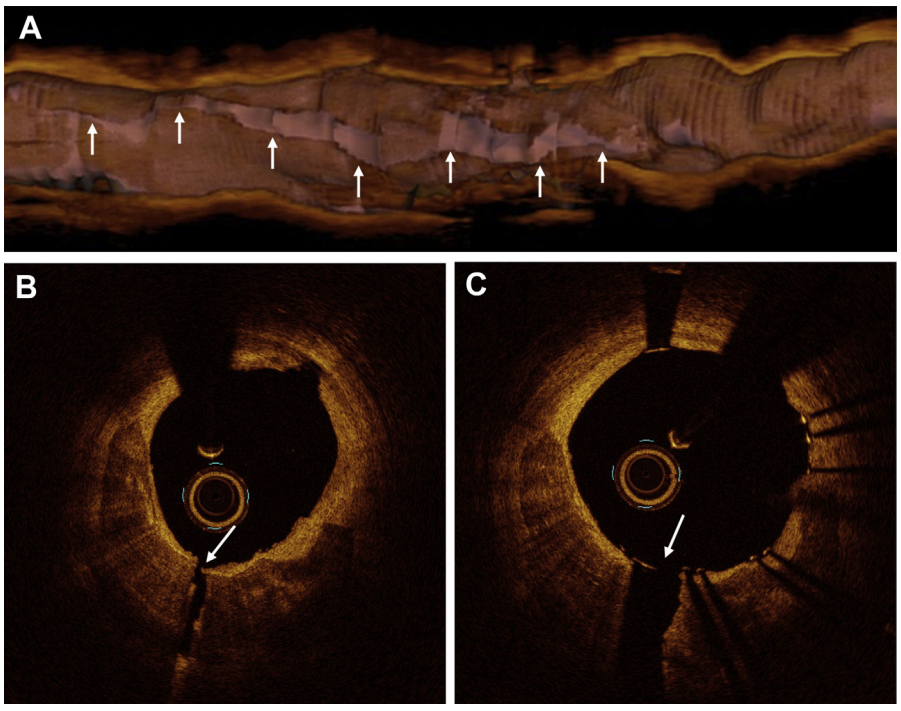

(A) Longitudinal image acquired post-stenting demonstrates longitudinal fracture displacement **(arrows)**. **(B)** Post-IVL OCT image demonstrates deep calcium fracture (1.09 mm) up to the adventitia. **(C)** Post-stent imaging demonstrates widening of the deep fracture (1.10 mm). Abbreviations as in **Figures 1 and 6**.

calcium thickness, regardless of calcium angle (52). Finally, a more robust analysis is forthcoming using patient-level pooled data from the Disrupt CAD I, Disrupt CAD II, Disrupt CAD III, and Disrupt CAD IV (Disrupt CAD IV With the Shockwave Coronary IVL System) OCT substudies (n = 250) to examine the effect of IVL treatment in eccentric and nodular calcium. Representative OCT images following IVL treatment in peripheral and coronary vessels are shown in **Figure 6**.

A consistent increase in vessel minimal luminal area was observed after low-pressure IVL balloon treatment in both peripheral and coronary vessels, suggesting improved vessel compliance following IVL-mediated calcium modification (30,52,53). Both circumferential and longitudinal calcium fractures in multiple planes were observed on OCT imaging following IVL treatment (**Figures 6 and 7**), and fracture width increased following stent expansion (30). These observations suggest that calcium fracture is the likely mechanism by which IVL enhances vessel compliance and facilitates optimal stent expansion. Although deep calcium fractures (to adventitia) have been observed following IVL treatment (**Figure 7**), which underscore the ability of IVL to modify deep vascular calcium, no vessel perforations were observed following IVL treatment alone in the Disrupt CAD and Disrupt PAD studies (28–30,52,58). The risk for vessel perforation is likely mitigated by the ability of IVL acoustic shockwaves to traverse soft tissue with minimal effect and by the presence of adventitial fibrosis, which has been demonstrated in advanced coronary and peripheral artery disease (59–62). Calcium fracture was observed in 67.7% of lesions after IVL in Disrupt CAD III. Interestingly, no differences were observed in minimal stent area, minimal luminal area, and stent expansion at the site of maximum calcification when comparing target lesions with or without demonstrable calcium fracture by OCT imaging (30). The apparent dissociation between the presence of calcium fracture demonstrated by OCT imaging and optimized indexes of stent implantation might be ascribed to fractures that were "out of plane" and not visualized or microfractures beyond the resolution of current OCT technology (63,64).

CENTRAL ILLUSTRATION **Intravascular Lithotripsy**

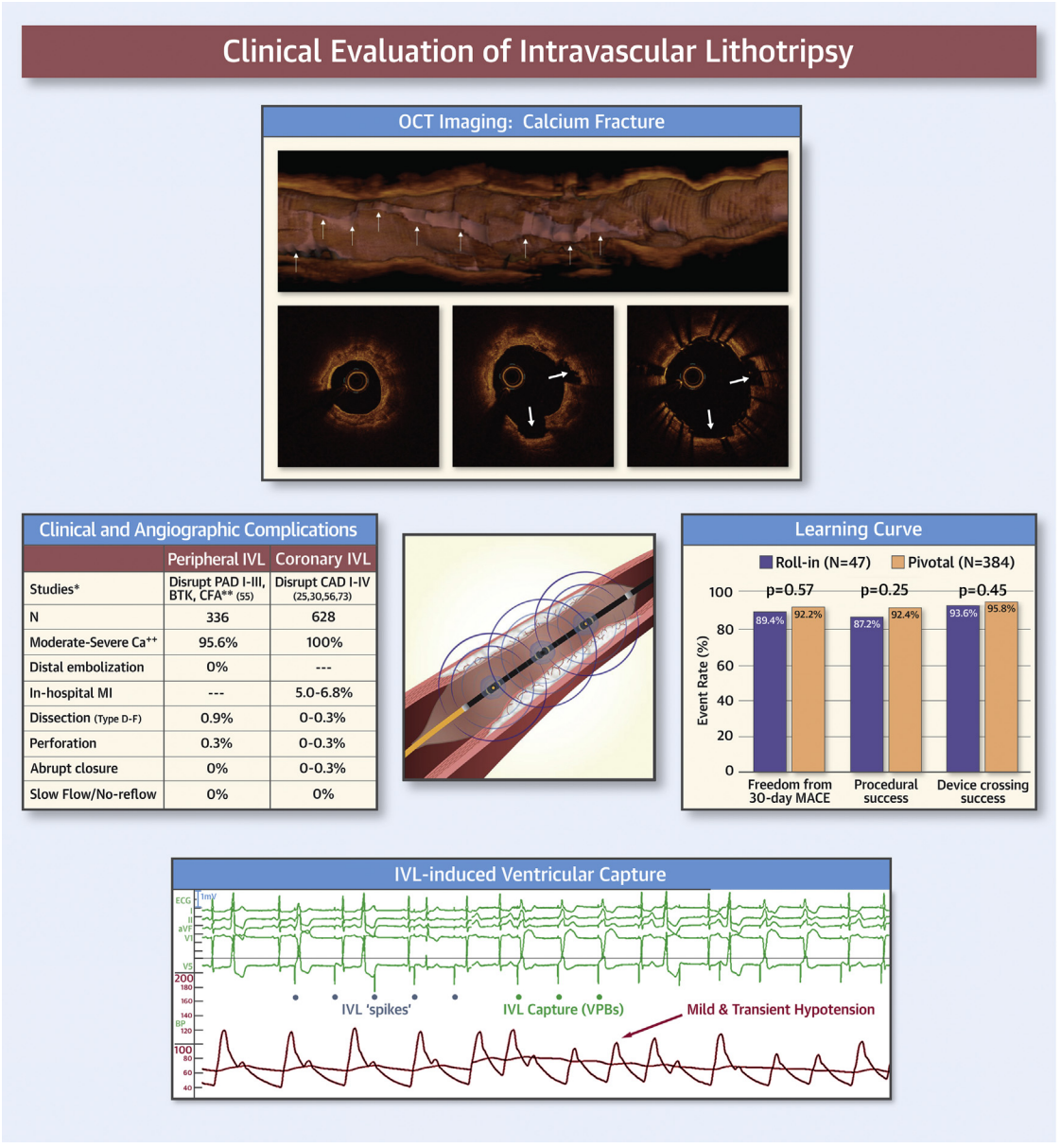

Kereiakes, D.J. et al. J Am Coll Cardiol Intv. 2021;14(12):1275–92.

Intravascular lithotripsy (IVL) which uses acoustic pressure waves to fracture vascular calcium has emerged as a novel treatment for patients with heavily calcified peripheral and coronary vessels. Multiple optical coherence tomographic (OCT) imaging sub-studies have demonstrated circumferential and longitudinal IVL-induced calcium fractures (denoted by **arrows** in representative OCT images), which facilitate stent expansion in severely calcified coronary vessels. IVL device ease-of-use was demonstrated in Disrupt CAD III, as safety and effectiveness outcomes were similar between the initial IVL procedure (roll-in) at each participating site and subsequent IVL procedures (pivotal). While IVL-induced ventricular capture has been observed (denoted by **green dots** in ECG tracing), primarily in bradycardic patients, these temporal events are usually benign without adverse sequelae. Clinical and angiographic complications remain low following IVL treatment of both peripheral and coronary calcified arteries. *All angiographic outcomes were adjudicated by an independent angiographic core laboratory. **Pooled patient-level analysis. OCT = optical coherence tomography.

FIGURE 8 Safety and Effectiveness Across the Disrupt CAD Studies

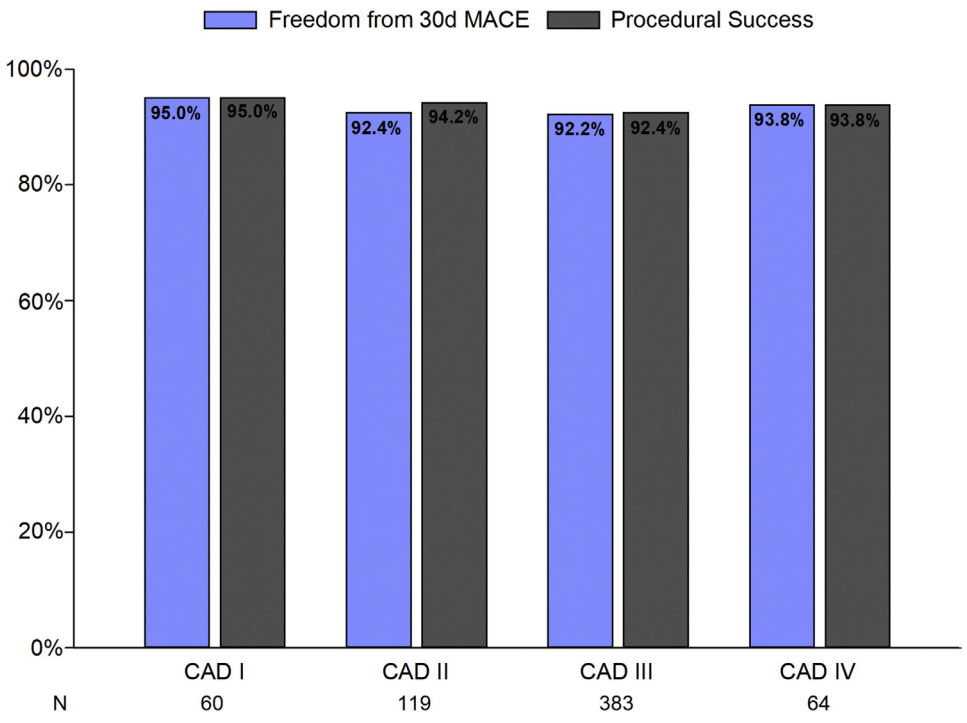

Freedom from 30-day major adverse cardiovascular events (MACE) is defined as freedom from the composite occurrence of cardiac death, myocardial infarction, or target vessel revascularization at 30 days. Procedural success is defined as successful stent delivery with a residual stenosis <50% by core laboratory assessment. CAD I = Shockwave Coronary Rx Lithoplasty Study; CAD II = Shockwave Coronary Lithoplasty Study; CAD III = Disrupt CAD III With the Shockwave Coronary IVL System; CAD IV = Disrupt CAD IV With the Shockwave Coronary IVL System.

EFFECT OF IVL ON SOFT TISSUE

HISTOPATHOLOGIC ANALYSIS. A histopathologic analysis examining the effect of IVL therapy (180 pulses over 6 cycles) delivery at 4-atm balloon inflation pressure on vascular injury and inflammation in porcine iliac and femoral arteries compared with treatment with balloon angioplasty alone was performed by an independent laboratory. Twenty-eight days after treatment, histomorphometric analysis was performed on arterial sections for the following parameters: tissue injury, inflammation, fibrin deposition, endothelialization, and neointimal smooth muscle content. Each parameter was graded on a scale of 0 to 3 according to previously published methodology (65). No differences were observed between the 2 treatment groups for any of the measured parameters, which supports the premise that IVL treatment has little effect on soft tissue (Supplemental Figure 7). Furthermore, no abnormalities were found in surrounding muscle tissue, which suggests that the impact of IVL treatment is limited to the vessel wall.

LOW VASCULAR COMPLICATION RATES WITH IVL. IVL therapy is balloon based, and therefore the risk for atheromatous embolization may be lower than observed following debulking atheroablative devices. Atherectomy devices often generate microparticulate debris that may embolize, causing distal microcirculatory occlusion with resultant slow or no reflow, tissue ischemia, and/or infarction. Fractured, larger calcium fragments generated by IVL appear to remain in situ. Indeed, an interim analysis of the "real-world" Disrupt PAD III observational study reported no distal embolization, no-reflow, or abrupt closure events (66) either with or without the use of embolic filters. Similarly, a pooled patient-level analysis (n = 336 patients) of peripheral IVL studies reported very low rates of perforation, distal embolization, no reflow, or abrupt closure (55). Furthermore, complex or flow-limiting dissections (types D to F) were rare, likely reflecting the lack of barotrauma following the low-pressure balloon inflations used during stand-alone IVL.

Similarly, the Disrupt CAD I and Disrupt CAD II trials demonstrated very low rates of coronary

TABLE 3 Angiographic Complications With Peripheral Calcium Modification Technologies

	IVL	Directional Atherectomy	Rotational Atherectomy	Orbital Atherectomy
Study	Patient-level pooled analysis: Disrupt PAD I, Disrupt PAD II, Disrupt PAD III, Disrupt BTK, Disrupt CFA (55)	DEFINITIVE Ca^{++} (19)	XL-PAD registry (21,75)	CONFIRM registries (76)
n	336	133	141, 26	3,135
Moderate to severe Ca^{++}, %	95.6	94.1%	14.4–100	81.1
Angiography core laboratory	Yes	Yes	Yes	No
Distal embolization, %	0.0	2.3*	8.0†	2.2
Dissection (types D-F), %	0.9	0.8	NR‡	NR§
Perforation, %	0.3	2.3	NR	0.7
Abrupt closure, %	0.0	NR	NR	1.5
Slow flow, %	0.0	NR	NR	4.4

Values are %, unless otherwise indicated. *97.2% embolic filter use with 88.4% of filters with captured debris. †Without embolic filter use. ‡27.3% reported for all dissections (75). §11.3% reported for all dissections.

DEFINITIVE Ca^{++} = Study of the SilverHawk/TurboHawk Plaque Excision Systems Used With SpiderFX to Treat Calcified Peripheral Arterial Disease; Disrupt BTK = Safety and Feasibility of the Shockwave Lithoplasty System for the Treatment of Peripheral Vascular Stenosis; Disrupt PAD I = Safety and Performance Study of the Shockwave Lithoplasty System; Disrupt PAD II = Shockwave Lithoplasty DISRUPT Trial for PAD; Disrupt PAD III = Shockwave Medical Peripheral Lithoplasty System Study for PAD; NR = not reported; XL-PAD = Multi-Center Registry for Peripheral Arterial Disease Interventions and Outcomes.

peri-procedural complications (rates of in-hospital myocardial infarction were 5.0% in Disrupt CAD I and 5.8% in Disrupt CAD II), with no unresolved complex dissections (types D to F), perforations, abrupt closures, and slow- or no-reflow events (25,56). The pivotal Disrupt CAD III trial demonstrated no perforations, abrupt closures, or no-reflow events following IVL alone despite treatment of more complex lesions than were treated in the Disrupt CAD I and Disrupt CAD II studies (30). Thus, in contrast to relatively high vascular complication rates observed after ESWL treatment, animal and core laboratory-adjudicated human clinical studies in both coronary and peripheral vessels suggest that IVL-related vascular complications are infrequent (**Central Illustration**).

IVL-INDUCED CAPTURE. IVL acoustic pressure waves have a pulse duration of 0.6 to 1.2 μs and are delivered at a rate of 1 Hz (1 pulse/s), with no electric component introduced to surrounding tissue. These acoustic pressure waves produce extremely low amounts of energy (8 to 10 μJ), which decay rapidly.

During coronary IVL treatment, ventricular ectopic activity or transient IVL-induced capture may occur and is dependent largely on resting heart rate. IVL-induced capture results from mechano-electric coupling of acoustic pressure waves with the cardiac conduction system that is mediated by cardiac stretch-activated channels used for conduction. Sustained ventricular capture is possible only when the acoustic pressure waves depolarize the cardiac tissue via the stretch-activated response and the native heart rate is lower than 60 beats/min, or R-R intervals vary to be >1 s. The resulting IVL-induced capture is at a rate of 60 beats/min for the duration of IVL treatment (10 s). Capture may be limited to single atrial capture, single ventricular capture, or ventricular capture sustained for more than 1 beat, but rarely more than for the 10-s duration of the IVL application.

The probability of ventricular tachycardia or ventricular fibrillation (VF) induction by IVL is remote considering that the 8 μJ (distributed over the surface of the C^2 IVL balloon) of mechanical energy applied is several orders of magnitude lower than that used in standard implantable cardioverter-defibrillator testing. In contrast, the electric energy required for ventricular tachycardia or VF induction during testing of a newly implanted implantable cardioverter-defibrillator is 0.6 to 2.0 J. Nevertheless, an isolated case report suggests the potential association of coronary IVL with VF induction but is confounded by the concurrent effects of balloon inflation-induced myocardial ischemia, spontaneous (not IVL related) ventricular ectopic effect on electric "vulnerability," and the use of IVL for an off-label indication (67). VF is a known risk in coronary diagnostic and interventional procedures, especially in the presence of underlying myocardial ischemia (68). Clearly, electrocardiographic monitoring is required during all coronary interventional procedures.

Wilson et al. (69) reported a high incidence of coronary IVL-induced pacing that was dependent largely on resting heart rate. Patients with heart rates <65 beats/min prior to IVL were 16-fold more likely (odds ratio: 16.3; 95% confidence

TABLE 4 Angiographic Complications With Coronary Calcium Modification Technologies

	IVL	Rotational Atherectomy	Orbital Atherectomy	Laser Atherectomy
Study	Disrupt CAD I, Disrupt CAD II, Disrupt CAD III, Disrupt CAD IV (25,30,56,73)	PREPARE-CALC (77)	ORBIT II (78)	Bilodeau et al. (79)
n	60, 120, 384, 64	100	443	95
Moderate to severe Ca^{++}, %	94.2-100	100	100*	80%†
Angiography core laboratory	Yes	Yes	Yes	Yes
In-hospital MI, %	5.0-6.8‡	2.0§	9.3‡	2.1
Dissection (types D-F), %	0.0-0.3	3.0||	0.9¶	5.3¶
Perforation, %	0.0-0.3	4.0	0.9	0.0
Abrupt closure, %	0.3	NR	0.2	0.0
Slow flow, %	0.0	2.0#	0.5	0.0
No reflow, %	0.0	–	0.0	–

Values are %, unless otherwise indicated. *Site reported. †Presence of calcium noted, but severity not specified. ‡CK-MB >3 times the upper limit of normal. §CK-MB >3 times the URL or troponin >3 times the URL. ||Large dissection (>5 mm). ¶Includes dissection types C to F. #Includes no reflow and slow flow.

CK-MB = creatine kinase myocardial band; Disrupt CAD I = Shockwave Coronary Rx Lithoplasty Study; Disrupt CAD II = Shockwave Coronary Lithoplasty Study; Disrupt CAD III = Disrupt CAD III With the Shockwave Coronary IVL System; Disrupt CAD IV = Disrupt CAD IV With the Shockwave Coronary IVL System; IVL = intravascular lithotripsy; MI = myocardial infarction; NR = not reported; ORBIT II = Evaluate the Safety and Efficacy of OAS in Treating Severely Calcified Coronary Lesions; PREPARE-CALC = Comparison of Strategies to Prepare Severely Calcified Coronary Lesions Trial; URL = upper reference limit.

interval: 2.4 to 110.8; p = 0.004) to experience IVL-induced capture compared with patients with heart rates ≥65 beats/min. No patient experienced sustained arrhythmias or clinically significant hypotension as a result of coronary IVL-induced capture, and all patients had successful percutaneous coronary intervention procedures without clinical sequelae.

To further evaluate this phenomenon, heart rhythm assessment was systematically performed in Disrupt CAD III (30). IVL-induced capture was observed in 41.1% of cases but did not result in sustained ventricular arrhythmias during or immediately after the IVL procedure and was not associated with adverse events. Multivariate Cox regression analysis identified heart rate ≤60 beats/min, male sex, and total number of IVL pulses delivered as independent predictors of IVL-induced capture. Although IVL-induced capture was relatively frequent, its occurrence was benign and without clinical consequence (30) (**Central Illustration**).

CLINICAL USE OF IVL

LEARNING CURVE ASSESSMENT. IVL technology leverages the familiarity of angioplasty balloon catheters used for coronary and peripheral intervention to provide a safe, effective, and intuitively understandable (operator-friendly) procedure when treating complex calcified lesions. In Disrupt CAD III, which represented the initial coronary IVL experience for U.S. interventional cardiologists, no significant differences were observed when comparing the 47 roll-in procedures (the first case at each international site) with the subsequent 384 intention-to-treat procedures with respect to procedural success, device crossing success, and 30-day freedom from major adverse cardiovascular events despite the marked complexity of lesions treated (30), which underscores the relative ease of IVL use.

IVL IN CLINICAL PRACTICE. The Shockwave M^5 and S^4 IVL catheters are approved for use in Europe, the United States, and additional countries globally for treatment of peripheral vascular disease. Safety and effectiveness have been demonstrated in multiple clinical studies in various peripheral vascular beds (Supplemental Table 1). A recent patient-level pooled analysis of 336 patients with moderate to severely calcified peripheral lesions undergoing IVL treatment demonstrated consistent reductions in residual luminal diameter stenosis after IVL treatment regardless of vessel bed, calcium severity, calcium distribution (eccentric or concentric), or patient risk subgroup (55). Increasing clinical experience is available regarding the use of IVL facilitation of large-bore catheter placement using transfemoral artery access for transcatheter aortic valve replacement, endovascular abdominal or thoracic aortic stent grafts, and mechanical cardiac support devices (e.g., Impella) (70–72). This experience suggests that a large portion of patients deemed unacceptable for transfemoral access can be successfully and safely "converted," obviating the need for alternative (frequently surgical) access with the attendant

morbidities of general anesthesia and prolonged hospitalization in addition to greater procedure related resource consumption. Furthermore, complications including perforation, complex dissection, and the need for unplanned "bail-out" stent placement following IVL to facilitate transfemoral access procedures are rare.

The Shockwave C^2 IVL catheter has been commercially available in Europe since 2018, following the completion of Disrupt CAD I (56), and is now available commercially in more than 49 countries. Disrupt CAD III (U.S. investigational device exemption pre-market study) and Disrupt CAD IV (Japanese pre-market study) completed enrollment in 2020 (30,73). In all Disrupt CAD trials, patients with stable ischemic heart disease and severely calcified target lesions were treated (Supplemental Table 2). Rates of safety and effectiveness were consistently high across all Disrupt CAD studies, as shown in **Figure 8**. All Disrupt CAD studies included independent core laboratory-adjudicated OCT substudies that demonstrated calcium fractures in multiple planes and confirmed calcium fracture as the dominant mechanism of action for increased vessel compliance after IVL treatment (25,52). Clinical experience with coronary IVL continues to expand with the use of IVL across a range of target lesion calcium phenotypes in varied anatomic and procedural scenarios (Supplemental Table 4). Although the optimal percutaneous coronary intervention strategy for calcified lesions is evolving, the recently developed Society for Cardiovascular Angiography and Interventions algorithm incorporates the use of calcium-modifying technologies including IVL with intravascular imaging in guiding treatment of these complex coronary lesions (74).

COMPARISON WITH OTHER CALCIUM-MODIFYING TECHNOLOGIES

In the treatment of severely calcified lesions, IVL offers several advantages compared with balloon-based technologies (i.e., high-pressure noncompliant and cutting/scoring balloons) and atheroablative technologies (rotational or orbital atherectomy). First, whereas balloon-based technologies are dependent on high static pressure for plaque modification, IVL uses acoustic shockwaves delivered through a semi-compliant balloon inflated to only 4 atm, thus avoiding high-pressure inflation with the consequent potential for barotrauma observed with conventional noncompliant balloons. Second, atheroablative technologies rely on localized debulking of superficial calcium, which subjects target vessels to thermal injury and vascular complications. Wire bias in their effect results in eccentric ruts or troughs with the risk for incomplete calcium modification. Furthermore, atheroablative technologies are limited in their ability to modify deep calcium in the absence of marked wire bias and/or larger device sizes, both of which may negatively affect procedure safety. Alternatively, IVL fractures both superficial and deep calcium in situ and minimizes the risk for vascular complications or thermal injury. Rates of vascular complications for peripheral and coronary calcium-modifying technologies used in heavily calcified target lesions are listed in **Tables 3 and 4**.

FUTURE DIRECTIONS

Shockwave IVL builds upon the principles of EHL used in kidney stone fragmentation with adaptations made for safety, effectiveness, and ease of use to treat vascular calcium. The IVL acoustic waveform adapted for intravascular use has been shown to obviate many of the vascular complications observed with lithotripsy used to treat urolithiasis. The combined evidence from preclinical (Ultracal 30 and cadaveric micro-CT) and clinical (Disrupt PAD and Disrupt CAD) studies consistently supports the concept that IVL modifies both superficial and deep calcium by producing multiplane, circumferential, and longitudinal calcium fractures with consequent enhancement of transmural vessel compliance and stent expansion. IVL's unique mechanism of action for calcium modification has consistently been associated with low rates of clinical and vascular-angiographic complications.

There are several areas of potential iteration and improvement to the IVL catheter system that may enhance the clinical utility of this technology. First, a reduction in device crossing profile and increased IVL catheter flexibility could improve deliverability across heavily stenotic or tortuous lesions. The current crossing profile is larger than standard angioplasty balloon catheters because of the integration of EHL emitters into the shaft of the IVL catheter. Crossing profile and flexibility affect delivery. Second, a longer IVL catheter shaft length could allow the treatment of more distal lesions, while larger IVL balloon sizes could facilitate optimal sizing relative to larger coronary (i.e., left main) and peripheral (i.e., common iliac) vessels. Thus, expansion of the current maximum balloon matrix for the Shockwave C^2 IVL catheter for coronary arteries (4.0 mm) and the S^4 (4.0 mm) and M^5 (7.0 mm) IVL catheters used for peripheral arteries would allow more optimal IVL

balloon-to-artery sizing with improved acoustic energy transfer. Last, an increase in the total number of pulses delivered per catheter might allow more patients to be treated with a single IVL catheter and could potentially reduce the time and cost of the procedure.

Although acute outcomes following IVL in severely calcified coronary lesions have been very promising to date, longer term follow-up is required to understand how these acute outcomes, particularly optimized stent expansion and minimal stent area, will affect late clinical results. Disrupt CAD III has planned 2-year follow-up and will provide longer term clinical outcome data with which to assess the impact of optimized stent implantation after the intracoronary use of IVL. Additional areas of interest and investigation with respect to modification of vascular calcification include patients with unstable coronary syndromes, ostial or bifurcation coronary lesions, treatment of in-stent restenosis or underexpanded coronary stents (69–73), severe calcification in upper extremity vessels (i.e., carotid, subclavian/axillary, innominate) and vein grafts, as well as the infrarenal aorta, radial, and brachial arteries. An investigator-sponsored "all-comers" registry is currently enrolling in Spain (REPLICA [Registry of Coronary Lithotripsy in Spain; NCT04298307], N = 400) and, following U.S. Food and Drug Administration approval of the Shockwave Coronary IVL System, a post-market approval study is being developed to use the American College of Cardiology National Cardiovascular Data Registry CathPCI Registry to provide insights into device safety and effectiveness in an expanded "real-world" patient population. Additional investigator-initiated randomized controlled pilot studies involving comparisons of IVL with cutting or scoring balloons (BALI [Balloon Lithoplasty for Preparation of Severely Calcified Coronary Lesions; NCT04253171], N = 200; CCS [Coronary Calcification Study; NCT04428177], N = 40) or rotational atherectomy and laser atherectomy (ROLLERCOASTER [Rotational Atherectomy, Lithotripsy or Laser for the Treatment of Calcified Stenosis; NCT04181268], N = 150) are planned to evaluate the safety and effectiveness of IVL compared with other calcium-modifying technologies in severely calcified coronary lesions prior to stent implantation. Evidence on the effectiveness of IVL treatment in eccentric and/or nodular calcification is limited as well, and a pooled analysis of the Disrupt CAD I, Disrupt CAD II, Disrupt CAD III, and Disrupt CAD IV OCT substudies is currently being performed to address these questions. Randomized clinical trials of IVL with other calcium-modifying therapies (i.e., high-pressure balloon, atheroablative technologies, laser atherectomy) are required to provide direct evidence regarding the relative safety and effectiveness of these therapies and guide algorithms for treatment of heavily calcified lesions in the coronary and peripheral vasculature. Similarly, the potential applications of IVL to severely calcified aortic valves, rheumatic mitral stenosis, and mitral annular calcification are areas of potential investigation.

FUNDING SUPPORT AND AUTHOR DISCLOSURES

Dr. Kereiakes is a consultant for SINO Medical Sciences Technologies, Boston Scientific, Elixir Medical, Svelte Medical Systems, Caliber Therapeutics/Orchestra Biomed, and Shockwave Medical; and is a stockholder in Ablative Solutions. Dr. Virmani has received grant, research, and clinical trial support from the National Institutes of Health, the Leducq Foundation, 480 Biomedical, 4C Medical, 4Tech, Abbott, Accumedical, Amgen, Biosensors, Boston Scientific, Canon USA, Cardiac Implants, Celonova, Claret Medical, Concept Medical, Cook, CSI, DuNing, Edwards Lifesciences, Emboline, Endotronix, Envision Scientific, Lutonix/Bard, Gateway, Lifetech, Limflo, MedAlliance, Medtronic, Mercator, Merrill, Microport Medical, Microvention, Mitralign, MitrAssist, NAMSA, Nanova, Neovasc, NIPRO, Novogate, Occulotech, OrbusNeich Medical, Phenox, Profusa, Protembis, Qool, ReCor Medical, Senseonics, Shockwave, Sinomed, Spectranetics, Surmodies, Terumo, Vesper, W.L. Gore, and Xeltis; and is a consultant for Abbott Vascular, Boston Scientific, Celenova, Cook Medical, CSI, Edwards Lifesciences, Bard BD, Medtronic, OrbusNeich Medical, ReCor Medical, SinoMedical Technology, Surmodics, Terumo, W.L. Gore, and Xeltis. Dr. Hokama is an employee of Shockwave Medical. Dr. Illindala is an employee of Shockwave Medical. Dr. Mena-Hurtado is a consultant for Abbott, Boston Scientific, Cook, Medtronic, Cardinal Health, and Optum Labs. Dr. Holden is a clinical investigator and medical advisory board member for Shockwave Medical. Dr. Hill reports fees and grant support from Abbott Vascular, Boston Scientific, Abiomed, and Shockwave Medical; and is a stockholder in Shockwave Medical. Dr. Lyden is a consultant to Boston Scientific, Abbott, Medtronic, Shockwave Medical, PQ Bypass, Intact, and Penumbra. Dr. Ali has received grants from the National Institutes of Health/National Heart, Lung, and Blood Institute, Abbott Vascular, and Cardiovascular Systems; has received personal fees from Amgen, AstraZeneca, and Boston Scientific; and holds equity in Shockwave Medical. All other authors have reported that they have no relationships relevant to the contents of this paper to disclose.

ADDRESS FOR CORRESPONDENCE: Dr. Dean J. Kereiakes, The Carl and Edyth Lindner Center for Research and Education at The Christ Hospital, 2123 Auburn Avenue, Suite 424, Cincinnati, Ohio 45219, USA. E-mail: dean.kereiakes@thechristhospital.com.

REFERENCES

1. Rocha-Singh KJ, Zeller T, Jaff MR. Peripheral arterial calcification: prevalence, mechanism, detection, and clinical implications. Catheter Cardiovasc Interv 2014;83:E212–20.

2. Mattesini A, Di Mario C. Calcium: a predictor of interventional treatment failure across all fields of cardiovascular medicine. Int J Cardiol 2017;231:97–8.

3. Lee MS, Shah N. The impact and pathophysiologic consequences of coronary artery calcium deposition in percutaneous coronary interventions. J Invasive Cardiol 2016;28:160–7.

4. Mori S, Yasuda S, Kataoka Y, Morii I, Kawamura A, Miyazaki S. Significant association of coronary artery calcification in stent delivery route with restenosis after sirolimus-eluting stent implantation. Circ J 2009;73:1856–63.

5. Kini AS, Vengrenyuk Y, Pena J, et al. Optical coherence tomography assessment of the mechanistic effects of rotational and orbital atherectomy in severely calcified coronary lesions. Catheter Cardiovasc Interv 2015;86:1024–32.

6. Wiemer M, Butz T, Schmidt W, Schmitz KP, Horstkotte D, Langer C. Scanning electron microscopic analysis of different drug eluting stents after failed implantation: from nearly undamaged to major damaged polymers. Catheter Cardiovasc Interv 2010;75:905–11.

7. Madhavan MV, Tarigopula M, Mintz GS, Maehara A, Stone GW, Genereux P. Coronary artery calcification: pathogenesis and prognostic implications. J Am Coll Cardiol 2014;63:1703–14.

8. Newman AB, Naydeck BL, Sutton-Tyrrell K, Feldman A, Edmundowicz D, Kuller LH. Coronary artery calcification in older adults to age 99: prevalence and risk factors. Circulation 2001;104:2679–84.

9. Tzafriri AR, Garcia-Polite F, Zani B, et al. Calcified plaque modification alters local drug delivery in the treatment of peripheral atherosclerosis. J Control Release 2017;264:203–10.

10. Genereux P, Madhavan MV, Mintz GS, et al. Ischemic outcomes after coronary intervention of calcified vessels in acute coronary syndromes. Pooled analysis from the HORIZONS-AMI (Harmonizing Outcomes With Revascularization and Stents in Acute Myocardial Infarction) and ACUITY (Acute Catheterization and Urgent Intervention Triage Strategy) TRIALS. J Am Coll Cardiol 2014;63:1845–54.

11. Yamamoto MH, Maehara A, Karimi Galougahi K, et al. Mechanisms of orbital versus rotational atherectomy plaque modification in severely calcified lesions assessed by optical coherence tomography. J Am Coll Cardiol Intv 2017;10:2584–6.

12. Abdel-Wahab M, Richardt G, Joachim Buttner H, et al. High-speed rotational atherectomy before paclitaxel-eluting stent implantation in complex calcified coronary lesions: the randomized ROTAXUS (Rotational Atherectomy Prior to Taxus Stent Treatment for Complex Native Coronary Artery Disease) trial. J Am Coll Cardiol Intv 2013;6:10–9.

13. Matsuo H, Watanabe S, Watanabe T, et al. Prevention of no-reflow/slow-flow phenomenon during rotational atherectomy—a prospective randomized study comparing intracoronary continuous infusion of verapamil and nicorandil. Am Heart J 2007;154:994.e1–6.

14. Fanelli F, Cannavale A, Gazzetti M, et al. Calcium burden assessment and impact on drug-eluting balloons in peripheral arterial disease. Cardiovasc Interv Radiol 2014;37:898–907.

15. Tepe G, Beschorner U, Ruether C, et al. Drug-eluting balloon therapy for femoropopliteal occlusive disease: predictors of outcome with a special emphasis on calcium. J Endovasc Ther 2015;22:727–33.

16. Kawaguchi R, Tsurugaya H, Hoshizaki H, Toyama T, Oshima S, Taniguchi K. Impact of lesion calcification on clinical and angiographic outcome after sirolimus-eluting stent implantation in real-world patients. Cardiovasc Revasc Med 2008;9:2–8.

17. Lee MS, Canan T, Rha SW, Mustapha J, Adams GL. Pooled analysis of the CONFIRM registries: impact of gender on procedure and angiographic outcomes in patients undergoing orbital atherectomy for peripheral artery disease. J Endovasc Ther 2015;22:57–62.

18. Babaev A, Zavlunova S, Attubato MJ, Martinsen BJ, Mintz GS, Maehara A. Orbital atherectomy plaque modification assessment of the femoropopliteal artery via intravascular ultrasound (TRUTH Study). Vasc Endovascular Surg 2015;49:188–94.

19. Roberts D, Niazi K, Miller W, et al. Effective endovascular treatment of calcified femoropopliteal disease with directional atherectomy and distal embolic protection: final results of the DEFINITIVE Ca^{++} trial. Catheter Cardiovasc Interv 2014;84:236–44.

20. McKinsey JF, Zeller T, Rocha-Singh KJ, Jaff MR, Garcia LA, for the DEFINITIVE LE Investigators. Lower extremity revascularization using directional atherectomy: 12-month prospective results of the DEFINITIVE LE study. J Am Coll Cardiol Intv 2014;7:923–33.

21. Banerjee A, Sarode K, Mohammad A, et al. Safety and effectiveness of the Nav-6 filter in preventing distal embolization during Jetstream atherectomy of infrainguinal peripheral artery lesions. J Invasive Cardiol 2016;28:330–3.

22. Powers CJ, Tinterow MM, Burpee JF. Extracorporeal shock wave lithotripsy: a study of renal stone differences. Kans Med 1989;90:19–22.

23. Cleveland RO, McAteer JA. Physics of shock-wave lithotripsy. In: Smith's Textbook of Endourology. Hoboken, NJ: Wiley-Blackwell, 2012:527–58.

24. Ali ZA, McEntegart M, Hill JM, Spratt JC. Intravascular lithotripsy for treatment of stent underexpansion secondary to severe coronary calcification. Eur Heart J 2020;41:485–6.

25. Ali ZA, Nef H, Escaned J, et al. Safety and effectiveness of coronary intravascular lithotripsy for treatment of severely calcified coronary stenoses: the Disrupt CAD II study. Circ Cardiovasc Interv 2019;12:e008434.

26. Brodmann M, Holden A, Zeller T. Safety and feasibility of intravascular lithotripsy for treatment of below-the-knee arterial stenoses. J Endovasc Ther 2018;25:499–503.

27. Brodmann M, Schwindt A, Argyriou A, Gammon R. Safety and feasibility of intravascular lithotripsy for treatment of common femoral artery stenoses. J Endovasc Ther 2019;26:283–7.

28. Brodmann M, Werner M, Brinton TJ, et al. Safety and performance of lithoplasty for treatment of calcified peripheral artery lesions. J Am Coll Cardiol 2017;70:908–10.

29. Brodmann M, Werner M, Holden A, et al. Primary outcomes and mechanism of action of intravascular lithotripsy in calcified, femoropopliteal lesions: results of Disrupt PAD II. Catheter Cardiovasc Interv 2019;93:335–42.

30. Hill JM, Kereiakes DJ, Shlofmitz RA, et al. Intravascular lithotripsy for treatment of severely calcified coronary artery disease. J Am Coll Cardiol 2020;76:2635–46.

31. Carlsson P, Kinn AC, Tiselius HG, Ohlsen H, Rahmqvist M. Cost effectiveness of extracorporeal shock wave lithotripsy and percutaneous nephrolithotomy for medium-sized kidney stones. A randomised clinical trial. Scand J Urol Nephrol 1992;26:257–63.

32. Peschel R, Janetschek G, Bartsch G. Extracorporeal shock wave lithotripsy versus ureteroscopy for distal ureteral calculi: a prospective randomized study. J Urol 1999;162:1909–12.

33. Lam JS, Greene TD, Gupta M. Treatment of proximal ureteral calculi: holmium:YAG laser ureterolithotripsy versus extracorporeal shock wave lithotripsy. J Urol 2002;167:1972–6.

34. Delacretaz G, Rink K, Pittomvils G, Lafaut JP, Vandeursen H, Boving R. Importance of the implosion of ESWL-induced cavitation bubbles. Ultrasound Med Biol 1995;21:97–103.

35. Wess OJ. Physics and technique of shock wave lithotripsy (SWL). In: Talai J, Tieselius HG, Albala DM, Ye Z, editors. Urolithiasis: Basic Science and Clinical Practice. London: Springer Verlag, 2012:301–11.

36. Rassweiler JJ, Knoll T, Kohrmann KU, et al. Shock wave technology and application: an update. Eur Urol 2011;59:784–96.

37. Lingeman JE, McAteer JA, Gnessin E, Evan AP. Shock wave lithotripsy: advances in technology and technique. Nat Rev Urol 2009;6:660–70.

38. McAteer JA, Evan AP. The acute and long-term adverse effects of shock wave lithotripsy. Semin Nephrol 2008;28:200–13.

39. Vorreuther R, Corleis R, Klotz T, Bernards P, Engelmann U. Impact of shock wave pattern and cavitation bubble size on tissue damage during ureteroscopic electrohydraulic lithotripsy. J Urol 1995;153:849–53.

40. Matlaga BR, McAteer JA, Connors BA, et al. Potential for cavitation-mediated tissue damage in shockwave lithotripsy. J Endourol 2008;22:121–6.

41. Scotland KB, Kroczak T, Pace KT, Chew BH. Stone technology: intracorporeal lithotripters. World J Urol 2017;35:1347–51.

42. Zheng W, Denstedt JD. Intracorporeal lithotripsy. Update on technology. Urol Clin North Am 2000;27:301–13.

43. Karimi Galougahi K, Patel S, Shlofmitz RA, et al. Calcific plaque modification by acoustic shockwaves: intravascular lithotripsy in coronary interventions. Circ Cardiovasc Interv 2021;14: e009354.

44. Li D, Pellegrino A, Hallack A, Petrinic N, Jerusalem A, Cleveland RO. Response of single cells to shock waves and numerically optimized waveforms for cancer therapy. Biophys J 2018; 114:1433–9.

45. McAteer JA, Williams JC Jr, Cleveland RO, et al. Ultracal-30 gypsum artificial stones for research on the mechanisms of stone breakage in shock wave lithotripsy. Urol Res 2005;33:429–34.

46. Pishchalnikov YA, McAteer JA, Williams JC Jr, Pishchalnikova IV, Vonderhaar RJ. Why stones break better at slow shockwave rates than at fast rates: in vitro study with a research electrohydraulic lithotripter. J Endourol 2006;20:537–41.

47. Dashwood MR, Noertersheuser P, Kirchengast M, Munter K. Altered endothelin-1 binding following balloon angioplasty of pig coronary arteries: effect of the ETA receptor antagonist, LU 135252. Cardiovasc Res 1999;43:445–56.

48. Gasser TC, Holzapfel GA. Modeling plaque fissuring and dissection during balloon angioplasty intervention. Ann Biomed Eng 2007;35:711–23.

49. Maglione J, Bergersen L, Lock JE, McElhinney DB. Ultra-high-pressure balloon angioplasty for treatment of resistant stenoses within or adjacent to previously implanted pulmonary arterial stents. Circ Cardiovasc Interv 2009;2:52–8.

50. Miller DL, Smith NB, Bailey MR, et al. Overview of therapeutic ultrasound applications and safety considerations. J Ultrasound Med 2012;31: 623–34.

51. O'Brien WD Jr. Ultrasound-biophysics mechanisms. Prog Biophys Mol Biol 2007;93:212–55.

52. Ali ZA, Brinton TJ, Hill JM, et al. Optical coherence tomography characterization of coronary lithoplasty for treatment of calcified lesions: first description. J Am Coll Cardiol Img 2017;10: 897–906.

53. Holden A. Safety and performance of the Shockwave Lithoplasty System in treating calcified peripheral vascular lesions: intravascular OCT analysis. Leipzig, Germany: LINC; 2018.

54. Isner JM, Donaldson RF, Fortin AH, Tischler A, Clarke RH. Attenuation of the media of coronary arteries in advanced atherosclerosis. Am J Cardiol 1986;58:937–9.

55. Madhavan MV, Shahim B, Mena-Hurtado C, Garcia L, Crowley A, Parikh SA. Efficacy and safety of intravascular lithotripsy for the treatment of peripheral arterial disease: an individual patient-level pooled data analysis. Catheter Cardiovasc Interv 2020;95:959–68.

56. Brinton TJ, Ali ZA, Hill JM, et al. Feasibility of Shockwave coronary intravascular lithotripsy for the treatment of calcified coronary stenoses: first description. Circulation 2019;139:834–6.

57. Blachutzik F, Honton B, Escaned J, et al. Safety and effectiveness of coronary intravascular lithotripsy in eccentric calcified coronary lesions: a patient-level pooled analysis from the Disrupt CAD I and CAD II studies. Clin Res Cardiol 2021; 110:228–36.

58. Gray W. Intravascular lithotripsy for peripheral artery calcification: the Disrupt PAD III randomized controlled trial 30-day outcomes. Available at: https://www.vivaphysicians.org/viva-programming 2020. Accessed March 23, 2021.

59. Cai WJ, Koltai S, Kocsis E, et al. Remodeling of the adventitia during coronary arteriogenesis. Am J Physiol Heart Circ Physiol 2003;284:H31–40.

60. Pasterkamp G, Galis ZS, de Kleijn DP. Expansive arterial remodeling: location, location, location. Arterioscler Thromb Vasc Biol 2004;24: 650–7.

61. Michel JB, Thaunat O, Houard X, Meilhac O, Caligiuri G, Nicoletti A. Topological determinants and consequences of adventitial responses to arterial wall injury. Arterioscler Thromb Vasc Biol 2007;27:1259–68.

62. Xu F, Ji J, Li L, Chen R, Hu W. Activation of adventitial fibroblasts contributes to the early development of atherosclerosis: a novel hypothesis that complements the "response-to-injury hypothesis" and the "inflammation hypothesis". Med Hypotheses 2007;69:908–12.

63. Wang X, Matsumura M, Mintz GS, et al. In vivo calcium detection by comparing optical coherence tomography, intravascular ultrasound, and angiography. J Am Coll Cardiol Img 2017;10:869–79.

64. Mori H, Torii S, Kutyna M, Sakamoto A, Finn AV, Virmani R. Coronary artery calcification and its progression: what does it really mean? J Am Coll Cardiol Img 2018;11:127–42.

65. Schwartz RS, Huber KC, Murphy JG, et al. Restenosis and the proportional neointimal response to coronary artery injury: results in a porcine model. J Am Coll Cardiol 1992;19:267–74.

66. Adams G, Shammas N, Mangalmurti S, et al. Intravascular lithotripsy for treatment of calcified lower extremity arterial stenosis: initial analysis of the Disrupt PAD III study. J Endovasc Ther 2020; 27:473–80.

67. McGarvey M, Kumar S, Violaris A, et al. Ventricular fibrillation induced by a lithotripsy-pulse on T during coronary intravascular shockwave lithotripsy. Eur Heart J Case Rep 2020;4:1–3.

68. Shaik FA, Slotwiner DJ, Gustafson GM, Dai X. Intra-procedural arrhythmia during cardiac catheterization: a systematic review of literature. World J Cardiol 2020;12:269–84.

69. Wilson SJ, Spratt JC, Hill J, et al. Incidence of "shocktopics" and asynchronous cardiac pacing in patients undergoing coronary intravascular lithotripsy. EuroIntervention 2020;15:1429–35.

70. Di Mario C, Goodwin M, Ristalli F, et al. A prospective registry of intravascular lithotripsy-enabled vascular access for transfemoral transcatheter aortic valve replacement. J Am Coll Cardiol Intv 2019;12:502–4.

71. Rosseel L, De Backer O, Sondergaard L, Bieliauskas G. Intravascular iliac artery lithotripsy to enable transfemoral thoracic endovascular aortic repair. Catheter Cardiovasc Interv 2020;95: E96–9.

72. Riley RF, Corl JD, Kereiakes DJ. Intravascular lithotripsy-assisted Impella insertion: a case report. Catheter Cardiovasc Interv 2019;93: 1317–9.

73. Saito S, Yamazaki S, Takahashi A, et al. Intravascular lithotripsy for vessel preparation in severely calcified coronary arteries prior to stent placement: primary outcomes from the Japanese Disrupt CAD IV study. Circ J 2021;85(6):826–33.

74. Riley RF, Henry TD, Mahmud E, et al. SCAI position statement on optimal percutaneous coronary interventional therapy for complex coronary artery disease. Catheter Cardiovasc Interv 2020; 96:346–62.

75. Maehara A, Mintz GS, Shimshak TM, et al. Intravascular ultrasound evaluation of JETSTREAM atherectomy removal of superficial calcium in peripheral arteries. EuroIntervention 2015;11:96–103.

76. Das T, Mustapha J, Indes J, et al. Technique optimization of orbital atherectomy in calcified peripheral lesions of the lower extremities: the CONFIRM series, a prospective multicenter registry. Catheter Cardiovasc Interv 2014;83:115–22.

77. Abdel-Wahab M, Toelg R, Byrne RA, et al. High-speed rotational atherectomy versus modified balloons prior to drug-eluting stent implantation in severely calcified coronary lesions. Circ Cardiovasc Interv 2018;11:e007415.

78. Chambers JW, Feldman RL, Himmelstein SI, et al. Pivotal trial to evaluate the safety and efficacy of the orbital atherectomy system in treating de novo, severely calcified coronary lesions (ORBIT II). J Am Coll Cardiol Intv 2014;7:510–8.

79. Bilodeau L, Fretz EB, Taeymans Y, Koolen J, Taylor K, Hilton DJ. Novel use of a high-energy excimer laser catheter for calcified and complex coronary artery lesions. Catheter Cardiovasc Interv 2004;62:155–61.

KEY WORDS calcification, coronary artery disease, intravascular lithotripsy, peripheral artery disease

APPENDIX For supplemental figures, a video, and tables, please see the online version of this paper.